Eur. Phys. J. E **8**, 339–346 (2002)
DOI 10.1140/epje/i2002-10019-y

THE EUROPEAN PHYSICAL JOURNAL E
EDP Sciences

Equilibrium charge distribution on annealed polyelectrolytes

T. Zito and C. Seidel[a]

Max-Planck-Institut für Kolloid- und Grenzflächenforschung, Am Mühlenberg, D-14476 Golm, Germany[b]

Received 7 March 2002 and Received in final form 28 May 2002

Abstract. Monte Carlo simulations are used to study the non-uniform equilibrium charge distribution along a single annealed polyelectrolyte chain under θ solvent conditions and with added salt. Within a range of the order of the Debye length charge accumulates at chain ends while a slight charge depletion appears in the central part of the chain. The simulation results are compared with theoretical predictions recently given by Castelnovo *et al.* In the parameter range where the theory can be applied we find almost perfect quantitative agreement.

PACS. 61.25.Hq Macromolecular and polymer solutions; polymer melts; swelling – 36.20.-r Macromolecules and polymer molecules – 05.20.-y Classical statistical mechanics

1 Introduction

The term polyelectrolyte is employed for the wide field of macromolecules which contain dissociable subunits (see, *e.g.*, [1,2] and references therein). With respect to different dissociation behavior one can distinguish between strong and weak polyelectrolytes [1] or between quenched and annealed ones [3]. So-called strong polyelectrolytes, polysalts as, *e.g.*, Na-polystyrene sulfonate, dissociate completely in the total pH range accessible by experiment. The total charge as well as its specific distribution along the chain is solely imposed by chemistry, *i.e.*, by polymer synthesis. That is why such polyelectrolytes are also called quenched. On the other hand, weak polyelectrolytes represented by polyacids and polybases dissociate only in a rather limited pH range. The total charge of the chain is not fixed but it can be tuned by changing the pH of the solution. Because of dissociation and recombination of ion pairs along the chain one expects spatial and/or temporal fluctuations in the local degree of dissociation. Such titrating polyelectrolytes exhibit an annealed inhomogeneous charge distribution. A pronounced charge accumulation appears at chain ends because there are fewer neighbors for the charges to interact with and the penalty in energy is therefore reduced. Although, at the level of scaling laws describing the statistical properties of polymer chains, the local charge distribution has only a weak effect on numerical pre-factors [2] the extra degree of freedom for the charges leads to new and non-trivial features. The charge inhomogeneity can have a strong impact on processes dominated by end-effects, such as the self-assembly of weakly charged linear micelles [4] and adsorption on charged surfaces [5]. For end-grafted weak polyelectrolytes, a rather unusual regime has been obtained where the chain stretching (brush thickness) depends non-monotonously on salt concentration [6] and grafting density [7]. This is mainly due to the fact that the net charge of a chain as well as its distribution along the chain is not fixed but depends on its local environment.

The dissociation of a low molecular acid (HA) in an aqueous medium is given by the equilibrium reaction

$$\mathrm{HA} + \mathrm{H_2O} \rightleftharpoons \mathrm{H_3O^+} + \mathrm{A^-},$$

or more simply by

$$\mathrm{HA} \rightleftharpoons \mathrm{H^+} + \mathrm{A^-}.$$

The law of mass action yields the equilibrium constant

$$K_\mathrm{a} = \frac{[\mathrm{H^+}]\,[\mathrm{A^-}]}{[\mathrm{HA}]}, \tag{1}$$

where $[\mathrm{A^-}]$, $[\mathrm{HA}]$, $[\mathrm{H^+}]$ are the (monomolar) concentrations of dissociated and undissociated acid and dissociated hydrogen, respectively. Using the standard notation $p\mathrm{H} = -\log_{10}[\mathrm{H^+}]$, $pK_\mathrm{a} = -\log_{10}[K_\mathrm{a}]$ and defining the degree of dissociation by

$$f = \frac{[\mathrm{A^-}]}{[\mathrm{HA}] + [\mathrm{A^-}]}, \tag{2}$$

equation (1) gives the well-known relation between the pH of the solution and degree of dissociation f of a simple acid

$$p\mathrm{H} = pK_\mathrm{a} + \log_{10}\left(\frac{f}{1-f}\right). \tag{3}$$

[a] e-mail: seidel@mpikg-golm.mpg.de
[b] Mailing address: D-14424 Potsdam, Germany.

The dissociation behavior of polyacids can be described in a similar way, but the resulting pK_a value is now an apparent one (in the physico-chemical literature denoted by pK_{app}) [8]. In contrast to low-molecular-weight acids, the charged groups of polyacids are linked together along the chain. Therefore, the dissociation of one acid group is correlated in a complex way to the position and the number of other charged groups of the chain resulting in a masking of the intrinsic pK_a^0 of a (polyelectrolyte) monomer. The corresponding relation can be written [3,9]

$$p\mathrm{H} = pK_a^0 + \log_{10}\left(\frac{f}{1-f}\right) + \frac{1}{N\,k_BT}\,\frac{\partial F_{el}}{\partial f}, \quad (4)$$

with F_{el} being the electrostatic free energy of the polyelectrolyte chain and N is the chain length. Introducing the chemical potential

$$\mu(f) = k_BT\log_{10}\left(\frac{f}{1-f}\right) + \frac{1}{N}\,\frac{\partial F_{el}}{\partial f}, \quad (5)$$

equation (4) can be written

$$p\mathrm{H} = pK_a^0 + \frac{1}{k_BT}\,\mu(f). \quad (6)$$

Clearly, the chemical potential has two contributions: i) an entropic one related to the mixing of charged and non-charged groups along the chain and ii) an electrostatic one related to the interaction with charged groups forming the local charge environment of an ionizable site. For good and θ solvents, the electrostatic contribution $\mu_{el}(f) = N^{-1}\,\partial F_{el}/\partial f$ is an increasing monotonic function of f. For poor solvents, Raphael and Joanny [3] found a non-monotonic variation of $\mu_{el}(f)$, and thus of $\mu(f)$, with f which results in a first-order phase transition from a collapsed weakly charged conformation to an extended strongly charged state.

The particular behavior of weak polyelectrolytes has attracted considerable interest in experimental [10–12], theoretical [3,13–16] and simulation [14,17–20] studies. Because a usual experimental approach to characterizing weak polyelectrolytes is to perform titration experiments, much effort has been done to understand the titration curves, *i.e.*, the dependence of the degree of ionization (or the degree of neutralization in the titration experiment) on the pH of the solution. The inhomogeneous charge distribution has been first studied by numerical simulation [14,19]. For not too large mean charge densities $\langle f\rangle$ and screening lengths λ_D, a quite good agreement between simulation data and the predictions of a linearized density-functional approach has been obtained in the case of rod-like polyelectrolytes [4,14]. Recently a generalization of the theory to the case of flexible chains has been given by Castelnovo *et al.* [16]. Qualitatively they found the result obtained in our previous simulations: a charge accumulation at chain ends. However, a quantitative comparison between theory and simulation data was not possible because the chains considered by Berghold *et al.* [14] are not in the asymptotic regime where the approach used in theory can be applied. A similar end-effect has been demonstrated in simulations of quenched strongly charged polyelectrolytes with explicit counterions: around the ends the counterion distribution is significantly different from that around the inner part of the chain [21]. However, although the resulting effective charge looks quite similar to that of an annealed polyelectrolyte, a quantitative comparison with the corresponding theoretical predictions is not possible due to some important differences between the two systems. So the theoretical predictions given by Castelnovo *et al.* are still waiting for a quantitative verification.

In the present paper we study the non-uniform charge distribution on annealed weakly charged polyelectrolytes in a θ solvent by (semi-)grand canonical Monte Carlo simulation. To be close to the theoretical model we consider chains where neighboring monomers are bound by harmonic springs. In addition, charged monomers interact with a Debye-Hückel potential, the screening length of which is tuned over the range where the theory is valid. In this case we observe not only qualitative agreement between simulation data and theory, but indeed a quite good quantitative one. Although the theoretical single-chain problem and its solution in a restricted parameter range may seem rather academic, it is a first step towards a more precise understanding of unusual collective properties of, *e.g.*, annealed polyelectrolyte brushes and stars.

The outline of the paper is as follows. In Section 2 we present the main theoretical predictions. The model and the method we use in the simulation are described in Section 3. In Section 4 we discuss the results and compare theory and simulation. Finally, a brief summary and our conclusions can be found in Section 5.

2 Theory

The free energy of an annealed, fully stretched polyelectrolyte chain (N monomers of size b) in a salty solution can be written as [22]

$$\frac{F}{k_BT} = \int_{-N/2}^{N/2} \mathrm{d}s \left\{ f(s)\left[\log\big(f(s)\big) - 1\right] - \mu\, f(s) + \frac{\lambda_B}{2}\int_{-N/2}^{N/2} \mathrm{d}s'\, f(s) f(s')\,\frac{\exp(-|s-s'|\,b/\lambda_D)}{|s-s'|\,b}\right\}, \quad (7)$$

where $f(s)$ is the local charge distribution along the chain. The Bjerrum length, which sets the strength of electrostatic interactions, is given by $\lambda_B = e^2/4\pi\varepsilon_0\varepsilon k_BT$ with e being the elementary charge and ε is the dielectric constant of the medium. Assuming a monovalent low-molecular electrolyte of concentration c_s, Debye screening length λ_D and Bjerrum length are related by $\lambda_D = (8\pi\lambda_B c_s)^{-1/2}$. The first term of equation (7) is the entropy of a unidimensional ideal gas, the second term fixes the charge on the chain by the chemical potential μ and the third term represents the electrostatic interaction between the charges on the chain. Note that one can justify the use of a Debye-Hückel potential only if the average

charge density $\langle f \rangle / b$ fulfills certain conditions: i) $\langle f \rangle$ has to be small to make non-linear effects unimportant, *i.e.*,

$$\langle f \rangle \frac{\lambda_{\mathrm{B}}}{b} = \langle f \rangle u < 1, \tag{8}$$

where we introduced the dimensionless parameter $u = \lambda_{\mathrm{B}}/b$, and ii) $\langle f \rangle$ has to be large to make sure that a sufficiently large number of charges interact simultaneously, *i.e.*,

$$\langle f \rangle \frac{\lambda_{\mathrm{D}}}{b} > 1. \tag{9}$$

Note that $\langle f \rangle \lambda_{\mathrm{B}}/b$ is the so-called Manning parameter for the condensation of counterions on a partially charged rigid rod.

Minimizing equation (7) the equilibrium charge density distribution on an annealed, fully stretched polyelectrolyte chain, up to first order in $\langle f \rangle \lambda_{\mathrm{B}}/b$, was found to be [14]

$$\frac{f(s)}{\langle f \rangle} = 1 + \langle f \rangle \frac{\lambda_{\mathrm{B}}}{b} \Bigg\{ E_1 \left[\left(\frac{N}{2} + s \right) \frac{b}{\lambda_{\mathrm{D}}} \right] + E_1 \left[\left(\frac{N}{2} - s \right) \frac{b}{\lambda_{\mathrm{D}}} \right] - 2 \frac{\lambda_{\mathrm{D}}}{Nb} \Bigg\}, \tag{10}$$

with the exponential integral $E_1(x) = \int_x^\infty \mathrm{d}t\, t^{-1} \exp(-t)$ [23]. Equation (10) gives a charge accumulation at the ends of the rod within a region of the order of the screening length. For a wide parameter range, the theoretical prediction was quantitatively confirmed by Monte Carlo simulations [14].

In order to study the charge distribution on a weakly charged, flexible polyelectrolyte chain, Castelnovo *et al.* [16] generalized equation (7) by including the entropy of a freely jointed chain. In the θ solvent case the free energy can be written as

$$\frac{F[\mathbf{r}_0(s)]}{k_{\mathrm{B}}T} = \int_{-N/2}^{N/2} \mathrm{d}s \Bigg\{ f(s) \left[\log\left(f(s)\right) - 1 \right] - \mu\, f(s) + \frac{3}{2b^2} \left(\frac{\mathrm{d}\mathbf{r}_0(s)}{\mathrm{d}s} \right)^2 + \frac{\lambda_{\mathrm{B}}}{2} \int_{-N/2}^{N/2} \mathrm{d}s'\, f(s) f(s') \times \frac{\exp\left[-|\mathbf{r}_0(s) - \mathbf{r}_0(s')|/\lambda_{\mathrm{D}} \right]}{|\mathbf{r}_0(s) - \mathbf{r}_0(s')|} \Bigg\}, \tag{11}$$

where $\mathbf{r}_0(s)$ denotes the so-called classical path of the polymer (the most probable conformation) which follows from the "chain-under-tension model" [24]. An important length scale which comes now into play is the electrostatic blob size ξ. From scaling arguments, *i.e.*, by equating the (unscreened) electrostatic interaction of the (quenched) charges inside one blob with $k_{\mathrm{B}}T$, one gets

$$\xi_{\mathrm{scaling}} = \frac{b}{\left(u f^2\right)^{1/3}}. \tag{12}$$

One blob contains $g = (\xi_{\mathrm{scaling}}/b)^2$ monomers and a chain of N monomers consists of

$$n_{\mathrm{b}} = N/g = N \left(u f^2\right)^{2/3} \tag{13}$$

electrostatic blobs. In order to reach the asymptotic regime one has to ensure that $n_{\mathrm{b}} \gg 1$. For a chain of finite length, however, the situation becomes even more complex. The electrostatic blob size varies along the chain resulting in a trumpet-like conformation with the maximum blob size at the chain ends. Up to a factor A the minimum blob size ξ_0 occurring in the middle of the chain is equal to ξ_{scaling} [16]. Later on we will use A as an adjustable parameter for comparison with simulation data. Using the rescaling relations given in reference [16] (Eqs. (36–39)), for a weakly charged chain of electrostatic blobs the conditions for applying the Debye-Hückel approximation, which correspond to equations (8, 9) discussed above, become

$$\langle f \rangle \frac{\lambda_{\mathrm{B}} \xi_0}{b^2} < 1, \tag{14}$$

and

$$\langle f \rangle \frac{\lambda_{\mathrm{D}} \xi_0}{b^2} > 1. \tag{15}$$

Thus, the Manning parameter reads now $\langle f \rangle \lambda_{\mathrm{B}}\, \xi_0/b^2 \sim \left(\langle f \rangle\, u^2\right)^{1/3}$. Note that the conditions imposed by applying the chain under tension model, *i.e.*, i) a fully flexible chain with $\xi_0 \gg b$ and ii) an aligned blob chain with $\lambda_{\mathrm{D}} \gg \xi_0$, are even stronger than those given in equations (14, 15). Specifically, assuming that

$$b \ll \xi_0 \ll \lambda_{\mathrm{D}} \ll L_{\mathrm{p}}, \tag{16}$$

where L_{p} is the persistence length (for inherently flexible chains due to electrostatic interaction), the solution of $f(s)$ up to first order in $\langle f \rangle \lambda_{\mathrm{B}}\, \xi_0/b^2$ was found to be very similar to equation (10) [16]:

$$\frac{f(s)}{\langle f \rangle} = 1 + \langle f \rangle \frac{\tilde{\lambda}_{\mathrm{B}}}{b} \Bigg\{ E_1 \left[\left(\frac{N}{2} + s \right) \frac{b}{\tilde{\lambda}_{\mathrm{D}}} \right] + E_1 \left[\left(\frac{N}{2} - s \right) \frac{b}{\tilde{\lambda}_{\mathrm{D}}} \right] - 2 \frac{\tilde{\lambda}_{\mathrm{D}}}{Nb} \Bigg\}, \tag{17}$$

with $\tilde{\lambda}_{\mathrm{B}}, \tilde{\lambda}_{\mathrm{D}}$ being Bjerrum and screening lengths expressed in terms of contour length

$$\tilde{\lambda}_{\mathrm{B}} = \frac{3\xi_0}{b} \lambda_{\mathrm{B}}, \tag{18}$$

$$\tilde{\lambda}_{\mathrm{D}} = \frac{3\xi_0}{b} \lambda_{\mathrm{D}}. \tag{19}$$

The relation between persistence length and screening length is a controversial problem which has been discussed for a couple of decades since the early work of Odijk, Skolnick and Fixman [25,26]. It is beyond the scope of the paper to go into details of that problem. Note that for fully flexible chains, the most recent results [27] confirm

Table 1. Systems studied and related scaling quantities ($N = 1000$, $u = \lambda_B/b = 0.9$).

$\langle f \rangle$	$\frac{\xi_{scaling}}{b}$	n_b	$\langle f \rangle \frac{\tilde{\lambda}_B}{b}$	$\frac{\lambda_D}{b}$	$\frac{\lambda_D}{\xi_{scaling}}$	$\frac{L_p^{KK}}{\lambda_D}$
				16	1.8	1.5
0.040	8.9	13	0.32	64	7.2	3.7
				256	28.8	16.7
				16	3.0	1.8
0.083	5.4	34	0.40	64	11.9	6.3
				256	47.4	25.0
				16	3.9	2.2
0.125	4.1	58	0.46	64	15.6	8.3
				256	62.4	30.9

the prediction for a chain of electrostatic blobs originally made by Khokhlov and Khachaturian [28]

$$L_p^{KK} \sim \xi_{scaling} + \frac{\lambda_D^2}{4\,\xi_{scaling}}. \tag{20}$$

Below we will use this relation to estimate the persistence length of the weakly charged chains considered in the simulations (see Tab. 1).

3 Simulation model and method

In the simulation the polyelectrolyte is represented by a freely jointed bead-spring chain, the realization of which we chose as close as possible to the model used in theory. Along the chain the N monomers are connected to their neighbors by a harmonic bond potential

$$U_{bond} = \frac{3}{2}\,k_B T \sum_{n=1}^{N-1} \frac{(\mathbf{r}_{n+1} - \mathbf{r}_n)^2}{b_0^2}, \tag{21}$$

with $\mathbf{r}_n$ being the position of bead n and b_0 is the (bare) average bond length, henceforth set equal to one. The thermal energy is $k_B T$. For convenience, we use $k_B T = 1$. All N_c (negatively) charged monomers interact *via* the Debye-Hückel potential

$$U_{DH} = \frac{k_B T}{2} \sum_{n \neq m=1}^{N_c} \frac{\lambda_B}{r_{nm}} \exp\left(-\frac{r_{nm}}{\lambda_D}\right), \tag{22}$$

where the Debye screening length λ_D is an input parameter. The exponentially decaying interaction enables the introduction of a cutoff which we chose as $\lambda_c = 5\,\lambda_D$. In the case of weakly charged polyelectrolytes in a θ solvent we study in the paper, average bond length as well as bond length distribution are only slightly effected by the electrostatic repulsion between charged monomers. Thus, the average bond length remains $b \approx b_0 = 1$. For water at room temperature, the Bjerrum length which gives the strength of the Coulomb interaction is about 7.14 Å. To avoid problems with counterion condensation, and to ensure that we work in a parameter range where the theory discussed above can be applied, we set the length scale by $u = \lambda_B/b = 0.9$. Then the Manning parameter of a chain of electrostatic blobs (see Eq. (14)) obeys $\langle f \rangle\, \lambda_B \xi_0/b^2 \sim \left(\langle f \rangle\, u^2\right)^{1/3} < 1$ by definition. With this setting of the length scale one has $b \approx 8$ Å. Hence, the polyelectrolyte chain is modeled on a coarse-grained level where one bead corresponds to a few chemical monomers. In the simulations reported here we consider a chain which consists of $N = 1000$ beads N_c of which carry an elementary charge. Because we study an annealed chain in a (semi-)grand canonical ensemble, N_c is not constant but only its average value $\langle N_c \rangle$ is fixed by the chemical potential μ. The chemical potential is chosen to result with an average degree of dissociation $\langle f \rangle = \langle N_c \rangle / N$ ranging from 1/25 to 1/8. The Debye screening length λ_D is varied over a range from 16 to 256 average bond lengths. With the setting of length scale introduced above, such screening lengths correspond to salt concentrations from 10^{-3}mol/L to 10^{-5}mol/L. Table 1 shows the systems studied by simulations together with the scaling quantities being of interest with respect to the conditions given in equation (16). One can see that the polyelectrolytes considered in the simulations at least fulfill the inequality relations which ensure that the chains reach the asymptotic regime assumed in theory. The conditions $n_b \gg 1$ and $\langle f \rangle\, \tilde{\lambda}_B / b \ll 1$ discussed in Section 2 are also reasonably fulfilled.

Equilibrium properties of the polyions are studied by standard Metropolis Monte Carlo (MC) [29] simulation. In order to guarantee the equilibration of both long- and short-length scales, bond angles and bond lengths we combine two different configurational MC moves: i) a pivot move where a monomer is chosen at random and the subsequent part of the chain is randomly rotated around that monomer, and ii) a local displacement move. The pivot algorithm was shown to be a highly efficient way to sample the phase space in a single-chain model with fixed bond lengths [30,31]. In the case of our freely jointed bead-spring model we found that the most efficient simulation route is a 1:1 mixing of the two MC moves. The correlation time of the mean-square end-to-end distance has been checked to be of the order of a few tens of MC steps. Thus, in any case we have correlation times below 0.1 Monte Carlo steps per monomer (MCM).

In order to simulate annealed polyelectrolytes, the MC simulation is performed in a (semi-)grand canonical ensemble where the chain is in contact with a reservoir of charges of fixed chemical potential μ. Additionally to the configurational MC moves introduced above the algorithm is completed with a charge move by which the charge state of a randomly chosen monomer is switched. Again a 1:1:1 combination of the three different MC moves was found to be the most efficient choice. The energy change of a complete MC move reads

$$\Delta E = \Delta E_c \pm \mu, \tag{23}$$

where ΔE_c is the change in configurational energy due to U_{bond} and U_{DH}. The plus sign is used when the monomer is

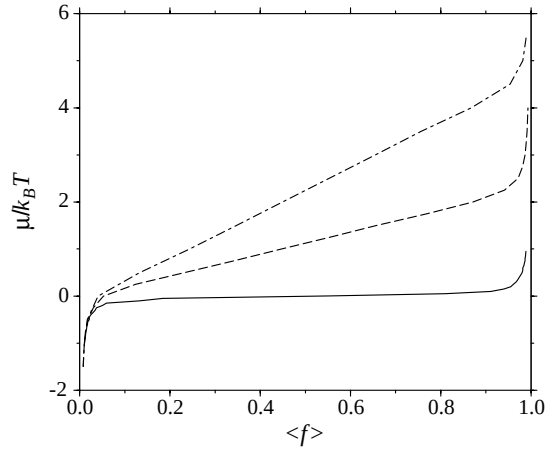

Fig. 1. Chemical potential μ *versus* average degree of dissociation $\langle f \rangle$ for a completely extended rigid chain at different Bjerrum lengths: $\lambda_B = 0$ (solid line), $\lambda_B = 0.5b$ (dashed line), $\lambda_B = 1.0b$ (dot-dashed line). Simulation results with $N = 100$, $\lambda_D = 10b$.

to be neutralized (protonated) and the minus sign when it is to be charged (deprotonated). Figure 1 shows the dependence between μ and average degree of dissociation $\langle f \rangle$ at different strength of Coulomb interaction, obtained by simulating a fully extended (rigid) polyelectrolyte. At vanishing interaction we have the ideal curve of isolated monomers. According to equation (6), μ/k_BT equals $p\mathrm{H} - pK_a^0$. Thus, Figure 1 represents the titration curves of the specific model. It might seem rather academic to study the behavior at different Bjerrum lengths. However, the important dimensionless parameter giving the strength of Coulomb interaction is $u = \lambda_B/b$. Hence, varying the average distance between ionizable groups b, which can be easily done during polyelectrolyte synthesis, one can succeed with a similar tuning of the strength of interaction as by varying λ_B.

Exploring different starting configurations, specifically a random one and the completely stretched one, the equilibration time of the chain was estimated to be $\tau_{equ} \approx 500$ MCM. To ensure sufficient relaxation, first the simulation is run for a time of at least 160 τ_{equ} which are about $80 \cdot 10^6$ MC steps. After reaching equilibrium, ensemble-averaged chain properties are taken as averages over at least $1.6 \cdot 10^4$ MCM, which corresponds to at least $1.6 \cdot 10^5$ renewal times. Note that we consider one MC step to be completed when the three partial steps (pivot move, local move, charge move) have been accepted. In this way the results on relevant quantities were found to be reproducible within a few percent.

Note a significant dependence of the acceptance rate on $\langle f \rangle$ and λ_D. We estimated it to range from about 60% for $\langle f \rangle = 0.040$, $\lambda_D = 16\,b$ down to about 20% for $\langle f \rangle = 0.125$, $\lambda_D = 256\,b$. Due to this difference CPU times between 16 hours and 9.5 days were necessary for performing simulation runs on Compaq Alpha machines with EV67/667 MHz processors.

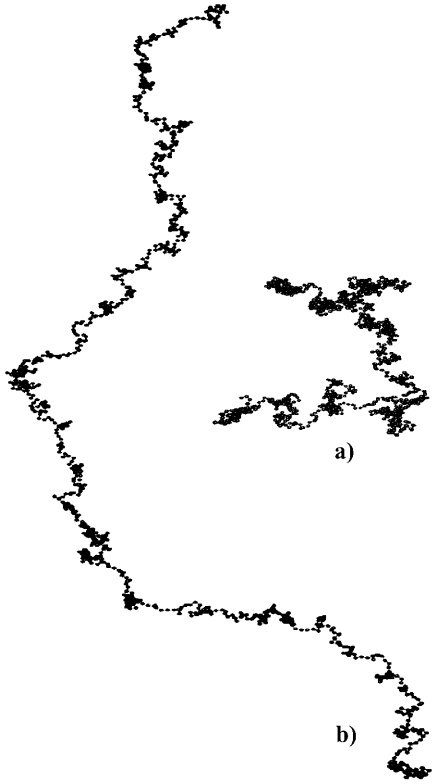

Fig. 2. Simulation snapshots of a partially charged chain ($N = 1000$, regularly quenched distribution with $f = 1/8$, θ solvent) at a) $\lambda_D = b$ and b) $\lambda_D = 500\,b$.

Table 2. Conformational properties of the systems studied: end-to-end distance R, radius of gyration R_g and shape factor R^2/R_g^2 ($N = 1000$, $u = \lambda_B/b = 0.9$).

$\langle f \rangle$	$\frac{\lambda_D}{b}$	$\frac{R}{b}$	$\frac{R_g}{b}$	$\frac{R^2}{R_g^2}$
0.040	16	62.8±0.3	23.6±0.1	7.1±0.1
	64	75.2±0.3	27.3±0.1	7.6±0.1
	256	77.4±0.3	28.0±0.1	7.6±0.1
0.083	16	98.0±0.4	35.5±0.1	7.6±0.1
	64	132.9±0.4	45.5±0.1	8.5±0.1
	256	143.5±0.3	48.5±0.1	8.8±0.1
0.125	16	129.3±0.4	46.1±0.1	7.9±0.1
	64	184.5±0.4	61.5±0.1	9.0±0.1
	256	206.2±0.4	67.4±0.1	9.4±0.1

4 Simulation results and comparison with theory

Table 2 shows conformational properties of the chains studied by simulations. As expected, the stretching of the chains is growing with increasing charge fraction $\langle f \rangle$ and/or screening length λ_D. The largest shape factor R^2/R_g^2 we obtain is 9.4. Remember that it ranges from 6 for a Gaussian chain up to 12 in the case of a rigid rod. For the largest screening length $\lambda_D = 256\,b$, we have always $\lambda_D > R$, *i.e.*, the electrostatic interaction

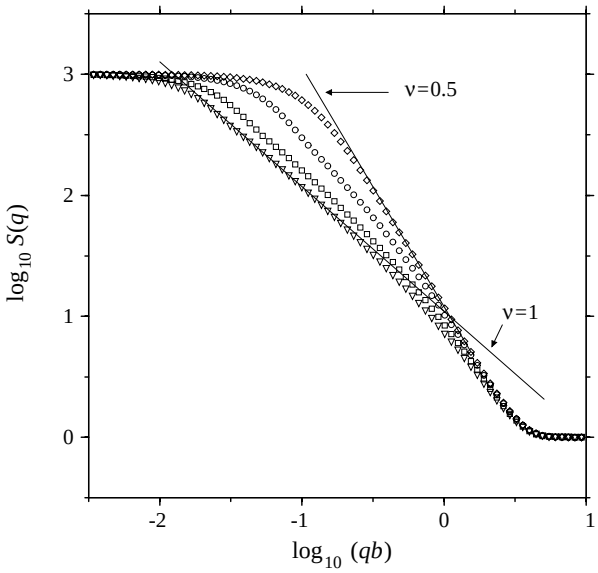

Fig. 3. Spherically averaged structure factor for partially charged chains ($N = 1000$, annealed charge distribution). Simulation results at varying degree of charging and screening length: $\langle f\rangle = 0.040, \lambda_{\rm D} = 16\,b$ (circles); $\langle f\rangle = 0.083, \lambda_{\rm D} = 64\,b$ (squares); $\langle f\rangle = 0.125, \lambda_{\rm D} = 256\,b$ (triangles). Additionally the result of an ideal chain is plotted (diamonds). The solid lines indicate asymptotic scaling laws.

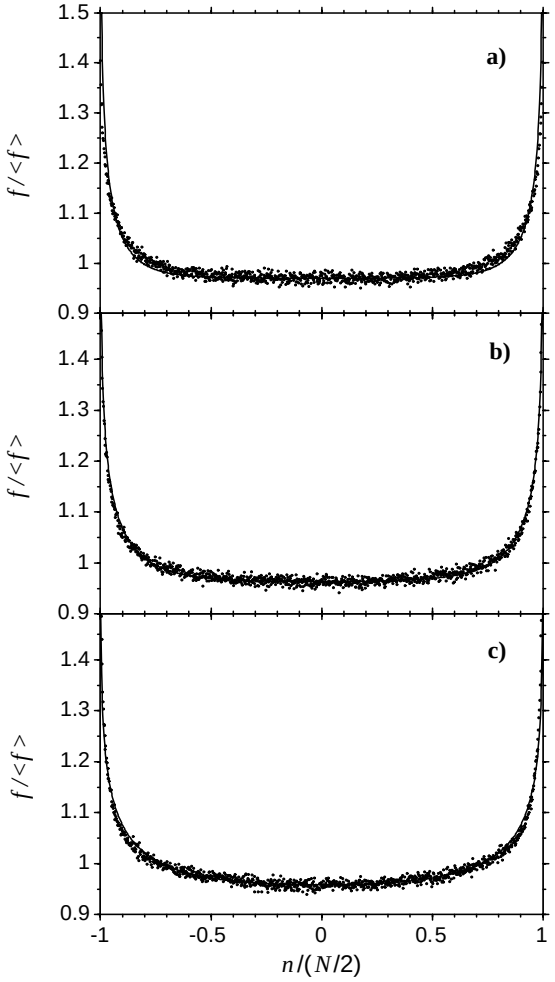

Fig. 4. Equilibrium charge distribution on annealed partially charged polyelectrolytes ($N = 1000$). Simulation results (symbols) and theoretical predictions (lines) at varying degree of charging and screening length: a) $\langle f\rangle = 0.040, \lambda_{\rm D} = 16\,b$, b) $\langle f\rangle = 0.083, \lambda_{\rm D} = 64\,b$, c) $\langle f\rangle = 0.125, \lambda_{\rm D} = 256\,b$.

is almost unscreened. Note that the effect of fluctuations in the charge distribution on large-scale mean statistical properties of free polyelectrolyte chains in dilute solutions is weak. In Figure 2 two typical simulation snapshots of a partially charged chain are shown where unite charges are regularly distributed with $f = 1/8$. The qualitative difference between the two snapshots, *i.e.* the polyelectrolyte effect, is not effected by charge annealing. In the high salt concentration case a), the Coulomb interaction is almost completely screened ($\lambda_{\rm D} = b$) and the configuration looks quite similar to a swollen coil in a good solvent. On the other hand, in the weak screening case b) we have an almost linear chain of blobs. At short-length scales, *i.e.* inside the blobs, there are coiled regions. At large-length scales the blobs appear to build a strongly elongated chain, the transverse extension of which is considerably smaller than the longitudinal one. An appropriate quantity that describes quantitatively the structure of the chain at all length scales is the single-chain structure factor or form factor. Here we calculate the spherically averaged structure factor

$$S(q) = \left\langle \left\langle \frac{1}{N} \left| \sum_{n=1}^{N} \exp(i\mathbf{q}\cdot\mathbf{r}_n) \right|^2 \right\rangle_{|\mathbf{q}|} \right\rangle . \qquad (24)$$

From the theory of uncharged polymers we know that the structure factor scales as $S(q) \sim q^{-1/\nu}$ in the range $2\pi/R < q < 2\pi/b$ with ν being the universal exponent for the mean extension of the chain $R \sim N^{\nu}$. The ideal chain and good solvent chain values of ν are $1/2$ and 0.588 ($\approx 3/5$), respectively. In Figure 3 $S(q)$ is plotted for three different systems with annealed charge distribution studied by simulation: i) at the minimum extension of the chain, ii) at a mean one and iii) at the maximum one (see Tab. 1). For large degree of charging and not too short screening lengths, linear scaling with $\nu \approx 1$ is reached at large length scales. On short scales we have an almost ideal random coil behavior. This is exactly the structure implied by the theory. Thus, in contrast to the previous simulations by Berghold *et al.* [14], now we expect a rather good agreement between simulation data and theory. In Figure 4 we show the corresponding charge distributions together with the theoretical predictions following from equation (17). We remind that the theory contains a free parameter A which sets the relation between the scaling theory blob size $\xi_{\rm scaling}$ and blob size in the middle of a finite chain $\xi_0 = A\,\xi_{\rm scaling}$. We fit A to obtain best agreement of the charge density at the middle of the chain where it forms an extended plateau. The resulting values of A are given in Table 3. In doing so, the agreement between simulation data and theoretical prediction is indeed almost perfect for the case where all the three inequalities

Table 3. Fitting of charge distribution $f(s)$ with the charge density in the middle of the chain $f(0)$. Values of parameter A.

λ_D/b	$\langle f \rangle$	$10 \times A$
	0.040	1.9
16	0.083	1.8
	0.125	1.6
	0.040	1.3
64	0.083	1.2
	0.125	1.2
	0.040	0.89
256	0.083	0.80
	0.125	0.76

given in equation (16) are fulfilled (case b) in Fig. 4). For decreasing charging (case a) in Fig. 4), the size of electrostatic blobs grows and becomes of the same order of magnitude as screening length (see Tab. 1). Then the interaction is too strongly screened to align the blob chain. At $\langle f \rangle = 0.040$, $\lambda_D = 16\,b$ the structure factor clearly shows (see Fig. 3) that the chain does not reach the asymptotic regime with $\nu \approx 1$ assumed in the theoretical model. Because of the stronger coiling, a longer part of the chain is packed within the range of a screening length which sets the spatial scale of the charge inhomogeneity. Thus, in agreement with simulation data we expect the charge to be accumulated in a larger chain section than predicted by theory. For strong charging (case c) in Fig. 4), the expansion parameter $\langle f \rangle \tilde{\lambda}_B/b$ becomes too large to justify a first-order perturbational treatment used in the theoretical approach discussed in Section 2. At this point we have to note that the fitting procedure of A described above is actually more complex than simply finding the right pre-factor of $\xi_{scaling}$ in the case of finite chain length. We remember that due to the restrictions of a first-order theory the normalization of the charge distribution $f(s)$ given by equations (10, 17) is correct in the limit $N \gg \lambda_B/b$ or $N \gg \tilde{\lambda}_B/b$, respectively. In reference [14] it has been shown that the first-order corrections due to finite-size effects give an additive constant in $f(s)$. Thus, the fitting of the free parameter A corrects not only for the unknown pre-factor of $\xi_{scaling}$ but also for the higher-order terms neglected in theory. However, doing so we obtain an almost perfect agreement between simulation data and theoretical predictions for the charge accumulation at chain ends within a length of the order of the Debye-Hückel screening length. From equations (17, 18) we know that, in first-order theory, the amplitude of charge inhomogeneity is proportional to the rescaled strength of interaction, *i.e.*, among others it is proportional to ξ_0. On the other hand, Table 3 shows that the relation between ξ_0 and $\xi_{scaling}$ is monotonously reduced with growing λ_D and/or $\langle f \rangle$. Thus, the larger screening length and degree of charging, the stronger becomes the correction of the (straightforward) first-order result. Actually, this tendency is in complete agreement with the behavior we obtained for rigid rods without introducing any fitting parameter [14]. With growing λ_D and f the first-order theory overestimates the inhomogeneity, but this error is compensated (at least partially) by the first correction term.

5 Conclusion

In this paper we reported (semi-)grand canonical Monte Carlo simulations of annealed weakly charged polyelectrolytes. In a fairly wide parameter range, *i.e.*, not too large mean charge densities $\langle f \rangle < b/\tilde{\lambda}_B$ and screening lengths in the range $\xi_{scaling} < \tilde{\lambda}_D < Nb$, we find a quite good quantitative agreement between simulation data and the results of the linearized theory recently proposed by Castelnovo *et al.* [16]. It would be interesting to have experimental evidence for the accumulation of charge at chain ends we obtain within a region of the order of the screening length. In order to being able to compare simulation data with theory, we have restricted the simulations to weakly charged polyelectrolytes ($\langle f \rangle \leq 0.125$). However, from previous simulations [14] it is known that the maximum of the overcharging at chain ends appears close to $\langle f \rangle \approx 0.5$, where the charge density at the ends can become about 50% higher than its mean value $\langle f \rangle$. In this case it should be possible to see experimentally the effect of the charge inhomogeneity on processes dominated by end-effects such as, *e.g.*, self-assembly of weakly charged micelles [4] and adsorption on charged surfaces [5]. But, such a charge density is clearly outside the range where the first-order theory is valid. Nonetheless the restricted theory, now for the first time proved by simulation data, is a step towards a more precise understanding of the more complex systems mentioned above.

We thank M. Castelnovo for helpful discussions and R. Netz for critical reading of the manuscript.

References

1. H. Dautzenberg, W. Jaeger, J. Kötz, B. Philipp, C. Seidel, D. Stscherbina, *Polyelectrolytes: Formation, Characterization and Application* (Hanser Publishers, Munich, Vienna, New York, 1994).
2. J.L. Barrat, J.-F. Joanny, Adv. Chem. Phys. **94**, 1 (1995).
3. E. Raphael, J.-F. Joanny, Europhys. Lett. **13**, 623 (1990).
4. P. van der Schoot, Langmuir **13**, 4926 (1997).
5. G.J. Fleer, M.A. Cohen Stuart, J.M.H.M. Scheutjens, T. Cosgrove, B. Vincent, *Polymers at Interfaces* (Chapman & Hall, London, Glasgow, New York, Tokyo, Melbourne, Madras, 1993).
6. R. Israels, F.A.M. Leermakers, G.J. Fleer, Macromolecules **27**, 3087 (1994).
7. E.B. Zhulina, T.M. Birshtein, O.V. Borisov, Macromolecules **28**, 1491 (1995).
8. A. Katchalsky, P. Spitnik, J. Polym. Sci. **2**, 432 (1947).
9. J.T.G. Overbeek, Bull. Soc. Chim. **57**, 252 (1948).
10. M. Mandel, in *Encyclopedia of Polymer Science and Engineering*, edited by H.F. Mark, N. Bikales, C.G. Overberger, G. Menges, J.I. Kroschwitz, 2nd edition, Vol. **11** (J. Wiley, New York, 1988) p. 739.
11. J. Kötz, B. Philipp, B. Pfannemüller, Makromol. Chem. **191**, 1219 (1990).
12. V. Tirtaatmadja, K.C. Tam, R.D. Jenkins, Macromolecules **30**, 3271 (1997).

13. B. Jönsson, M. Ullner, C. Peterson, O. Somelius, B. Söderberg, J. Phys. Chem. **100**, 407 (1996).
14. G. Berghold, P. van der Schoot, C. Seidel, J. Chem. Phys. **107**, 8083 (1997).
15. I. Borukhov, D. Andelman, R. Borrega, M. Cloitre, L. Leibler, H. Orland, J. Phys. Chem. B **104**, 11027 (2000).
16. M. Castelnovo, P. Sens, J.-F. Joanny, Eur. Phys. J. E **1**, 115 (2000).
17. C.E. Reed, W.F. Reed, J. Chem. Phys. **96**, 1609 (1992).
18. A.P. Sassi, S. Beltrán, H.H. Hooper, H.W. Blanch, J.M. Prausnitz, R.A. Siegel, J. Chem. Phys. **97**, 8767 (1992).
19. M. Ullner, B. Jönsson, B. Söderberg, C. Peterson, J. Chem. Phys. **104**, 3048 (1996).
20. M. Ullner, B. Jönsson, Macromolecules **29**, 6645 (1996).
21. H.J. Limbach, C. Holm, J. Chem. Phys. **114**, 9674 (2001).
22. J.P. Hansen, I.R. McDonald, *Theory of Simple Liquids* (Academic Press, London, 1986).
23. M. Abramowitz, I.A. Stegun, *Handbook of Mathematical Functions* (Dover Publications, New York, 1965).
24. J.L. Barrat, J.-F. Joanny, Europhys. Lett. **24**, 333 (1993).
25. T. Odijk, J. Polym. Sci., Polym. Phys. Ed. **15**, 477 (1977).
26. J. Skolnick, M. Fixman, Macromolecules **10**, 944 (1977).
27. R.R. Netz, H. Orland, Eur. Phys. J. B **8**, 81 (1999).
28. A.R. Khokhlov, K.A. Khachaturian, Polymer **23**, 1742 (1982).
29. N.A. Metropolis, A.W. Rosenbluth, M.N. Rosenbluth, A. Teller, E. Teller, J. Chem. Phys. **21**, 1087 (1953).
30. M. Lal, Mol. Phys. **17**, 57 (1969).
31. N. Madras, A.D. Sokal, J. Stat. Phys. **50**, 109 (1988).